Inorganic Chemistry

Article

pubs.acs.org/IC

Synthesis and Porous Properties of Chromium Azolate Porous Coordination Polymers

Kanokwan Kongpatpanich,[†] Satoshi Horike,*[,†,‡] Masayuki Sugimoto,[†] Tomohiro Fukushima,[†] Daiki Umeyama,[†] Yosuke Tsutsumi,[†] and Susumu Kitagawa*[,†,§]

[†]Department of Synthetic Chemistry and Biological Chemistry, Graduate School of Engineering, Kyoto University, Katsura, Nishikyo-ku, Kyoto 615-8510, Japan

[‡]Japan Science and Technology Agency, PRESTO, 4-1-8, Honcho, Kawaguchi, Saitama 332-0012, Japan

[§]Institute for Integrated Cell-Material Sciences (iCeMS), Kyoto University, Yoshida, Sakyo-ku, Kyoto 606-8501, Japan

Supporting Information

ABSTRACT: We developed a new route for synthesis of Cr-based porous coordination polymers (PCPs) with azole ligands and characterized the unique open structures by single-crystal X-ray studies and other spectroscopy techniques. Chromium-based PCPs have been prepared from azolate ligands 3,5-dimethyl-1*H*-pyrazole-4-carboxylic acid (H_2dmcpz) and 1,4-di(1*H*-tetrazole-5yl)benzene (H_2BDT) by solvothermal reactions under an Ar atmosphere. $[Cr_3O(Hdmcpz)_6(DMF)_3]\supset$DMF (**1**⊃DMF) is a coordination compound that forms a hydrogen-bonded porous network. $[Cr_3O(HBDT)_2(BDT)Cl_3)]\supset$DMF (**2**⊃DMF) possesses a new type of trinuclear chromium μ_3-O unit cluster and the novel topology of a Cr-based PCP with 700 $m^2\ g^{-1}$ of Brunauer–Emmett–Teller surface area. [Cr(BDT)(DEF)]⊃DEF (**3**⊃DEF) is structurally flexible and reactive to O_2 molecules because of the unsaturated Cr^{2+} centers. This is the first report of a Cr-based PCP/metal–organic framework with noncarboxylate ligands and characterization by single-crystal X-ray diffraction.

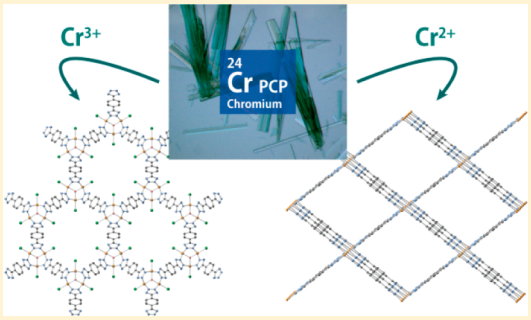

INTRODUCTION

Porous coordination polymers (PCPs) or metal–organic frameworks (MOFs) have been studied extensively because of the rich structures and functions that can be obtained from various choices of building unit: metal centers and organic linkers.[1] In general, the choice of metal ion has been biased toward the late first-raw transition metals such as Co^{2+}, Ni^{2+}, Cu^{2+}, and Zn^{2+}. Recently, the variety of metal ions has increased. For example, Ti^{3+}, Zr^{4+}, Ru^{2+}, and Ba^{2+} have been employed to construct the frameworks with unique structures and properties.[2] Among the metal ions available, the Cr-based PCP (mostly Cr^{2+} or Cr^{3+}) is still in its infancy due to synthetic difficulties, including the air-sensitive nature and the high reactivity of Cr^{2+} species. There are only a few families of Cr-based PCPs that show permanent porosity for gas adsorption, and all of the reported compounds are constructed from carboxylate ligands.[3] Note that, all Cr-based PCPs have been synthesized as microcrystalline powder, which in turn limits the understanding on the structure by single-crystal X-ray analysis. Postsynthetic metathesis of the metal node appears to be the only option to prepare Cr-based PCPs in single-crystal form,[4] but stoichiometric metal exchange is sometimes not feasible. It therefore remains a challenge in the field of PCPs to synthesize a Cr-based PCP from noncarboxylate ligands and to characterize the structure by single-crystal analysis to explore the unique functions derived from Cr ions in the open frameworks.

In this study, we synthesized three types of single crystals: two Cr PCPs and one hydrogen-bonded network of the discrete Cr coordination compound by using azolate ligands. These compounds can be prepared only under air-free conditions, and the porous structures are stable in air once these are constructed. Because of the combination of Cr and azolates, we observed a new type of trinuclear Cr cluster, structural flexibility, and O_2 binding property by Cr unsaturated coordination sites in the frameworks.

RESULTS AND DISCUSSION

Two types of azole ligands were selected with different acidity and coordination versatility. 3,5-Dimethyl-1*H*-pyrazole-4-carboxylic acid (H_2dmcpz)[5] contains a pyrazole ring and a carboxylic acid group. The reaction of $[(CH_3CO_2)_2Cr{\cdot}H_2O]_2$ and H_2dmcpz ligand under inert conditions yielded the bright green crystalline product $[Cr_3O(Hdmcpz)_6(DMF)_3]\supset$DMF (**1**⊃DMF), where DMF is *N*,*N*-dimethylformamide. Only the O atoms of the carboxylate group coordinate to the Cr center in the crystal structure of **1**⊃DMF (Figure 1a). Although the coordination bond between the metal and nitrogen tends to be more robust than the labile metal–oxygen bond,[6] the formation of the Cr–O bond is more favored in the self-assembly of

Received: June 20, 2014
Published: August 22, 2014

   dx.doi.org/10.1021/ic501459m | *Inorg. Chem.* 2014, 53, 9870–9875

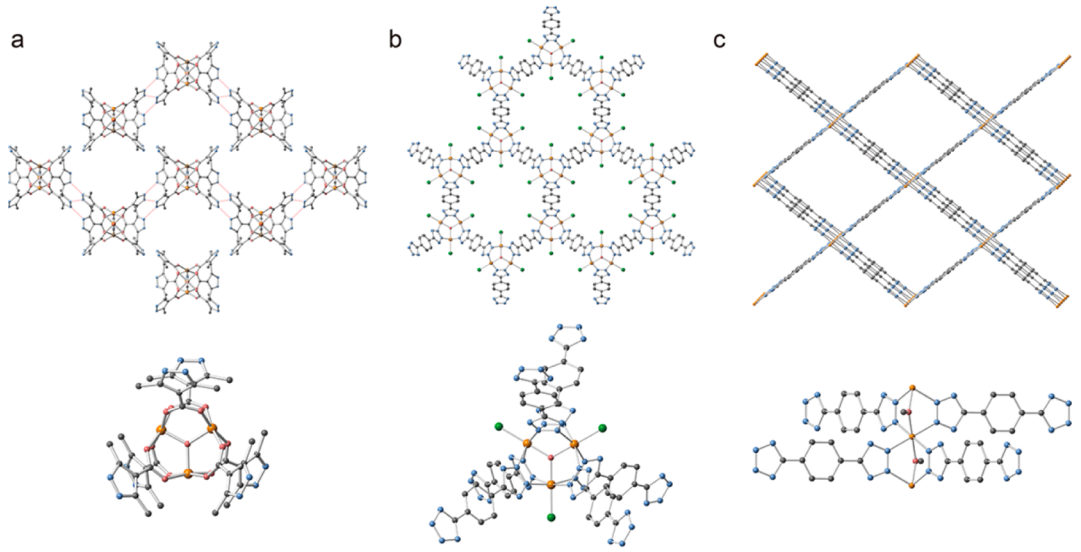

Figure 1. (a) Extended structure along the [001] direction and coordination environment in **1**⊃DMF. Hydrogen bonds are shown as a red dot line. (b) Extended structure along the [001] direction and the coordination environment in **2**⊃DMF. (c) Extended structure along the [010] direction and the coordination environment in **3′**⊃DEF. Orange, gray, blue, red, and green spheres represent Cr, C, N, O, and Cl atoms, respectively.

1⊃DMF. The crystal structure shows that **1**⊃DMF is a discrete coordination compound and can be classified as the trinuclear chromium basic acetate structure with the general formula $[M_3O(OOCR)_6L_3]$, where L is the ligand at the axial position.[7] **1**⊃DMF is a triangle of three Cr atoms with an O atom at the center. Each Cr atom coordinates to the bridging carboxylate groups at the equatorial positions and an O atom from the solvent at the axial position. The distance between the pyrazole N atoms of the two neighboring units is reasonable for the H bond (shown as red dots in Figure 1a).[8] Each unit is linked by intermolecular hydrogen bonds to form a porous network.

Tetrazole is an N-donor ligand with an acidity comparable to those of carboxylate ligands.[9] 1,4-Di(1*H*-tetrazole-5yl)benzene (H_2BDT) was chosen as a ligand to demonstrate the possibility of preparing crystals with a suitable size for single-crystal X-ray diffraction measurement. We synthesized $[Cr_3O(HBDT)_2(BDT)Cl_3)]$⊃DMF (**2**⊃DMF) from $CrCl_2$ under the same synthetic conditions as for **1**⊃DMF. The crystal structure reveals that **2**⊃DMF crystallizes in the hexagonal space group *P*63/*mmc* and contains trinuclear chromium oxo-centered clusters in the structure (Figure 1b). Trinuclear chromium basic acetate structures with the general formula ($[Cr_3O(OOCR)_6]$) clusters have been studied for decades,[7b,10] but the replacement of the carboxylate ligands with N-donor ligands has not been explored.[11] Each Cr in the Cr_3 cluster coordinates to four N atoms from tetrazolate moieties and one chloride atom in the axial position to create the extended structure. The packing structure of **2**⊃DMF has two different cavities, namely, the honeycomb-like channels along the [001] direction (Figure 1b) and the one-dimensional rhombic channels in the other directions. The overall topology is unique when compared to other PCPs prepared from the same ligand.[12]

The oxidation state of the Cr ions in the structure was investigated by X-ray photoelectron spectroscopy (XPS). The peak assigned for the Cr $2p_{3/2}$ state was fit with a binding energy of 577.7 eV (Figure 2a), which is assigned to Cr^{3+}.[13]

Even though the compound was prepared from $CrCl_2$, Cr^{2+} ions are likely to be oxidized to Cr^{3+} during the synthesis. We propose that a labile Cr^{2+} precursor is necessary to initiate the

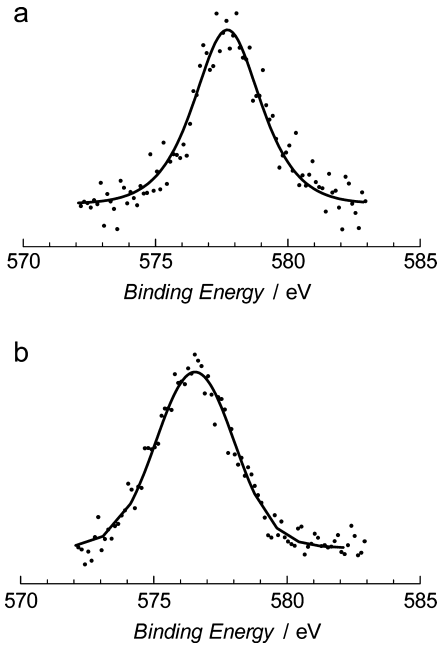

Figure 2. Cr $2p_{3/2}$ XPS spectra for (a) **2**, binding energy was fit to be 577.7 eV, and (b) **3′**, binding energy was fit to be 576.5 eV.

Cr−N bond formation. The coordinated chloride ions are probably involved in the stabilization of the overall framework and result in the oxidation of Cr^{2+} to Cr^{3+} during the synthesis. The use of a labile Cr^{2+} precursor instead of an inert Cr^{3+} precursor leads to the formation of a crystalline network. When the same reaction was conducted with $CrCl_3$, only noncrystalline solids were obtained.

We changed the Cr^{2+} precursor and obtained another compound under similar synthetic conditions of **2**⊃DMF. [Cr(BDT)(DEF)]⊃DEF (**3**⊃DEF) was prepared by the reaction of $[(CH_3CO_2)_2Cr{\cdot}H_2O]_2$ and H_2BDT in *N*,*N*-diethylformamide (DEF). The compound is air-sensitive, as evidenced by the color change from the original purple to dark beige within seconds in the air, which suggests a spontaneous

dx.doi.org/10.1021/ic501459m | *Inorg. Chem.* 2014, 53, 9870−9875

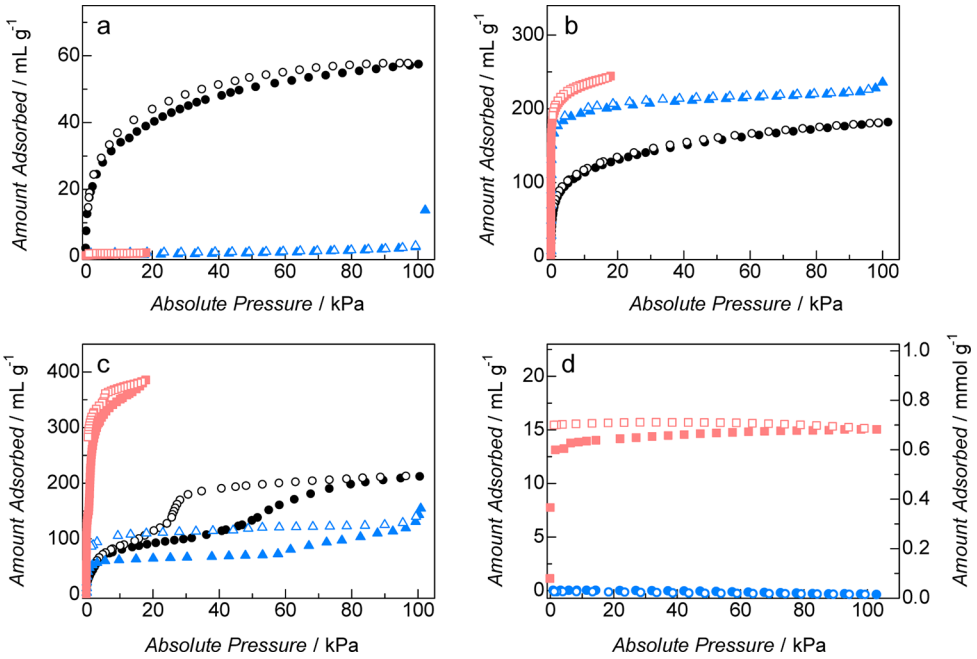

Figure 3. Adsorption (filled symbols) and desorption (open symbols) isotherms of (a) **1** (b) **2** (c) **3** for N_2 at 77 K (blue triangles), O_2 at 77 K (red squares), and CO_2 at 195 K (black circles), respectively. (d) O_2 (red squares) and N_2 isotherms (blue circles) of **3** measured at 298 K.

oxidation process. The rapid oxidation makes it is impossible to measure the totally air-free sample by single-crystal X-ray diffraction. Therefore, we reported only the crystal structure of the air-exposed sample (**3′**⊃DEF). Single-crystal analysis of **3′**⊃DEF, reveals a different topology from **2**⊃DMF (Figure 1b, c). Compound **3′**⊃DEF crystallizes in the orthorhombic space group *Imma*. The building unit is an infinite Cr chain *trans*-bridged by an O atom of solvent along the [010] direction (Figure 1c). These Cr chains are cross-linked with N2 and N3 atoms of the BDT^{2-} ligand in a bis-monodentate fashion to form a three-dimensional framework. The packing structure illustrates the one-dimensional rhombic channels along the [010] direction. The structure before air-exposure (**3**⊃DEF) was estimated from a LeBail analysis of the X-ray powder diffraction (XRPD) data (Figure S1, Supporting Information), and the analysis reveals similar structures with a change in the *b* parameter, which is the direction along the infinite Cr chains (*b* = 7.202 and 6.507 Å for **3**⊃DEF and **3′**⊃DEF, respectively).

An attempt was made to determine the chemical state of Cr by XPS analysis. However, we were unable to prepare the air-free sample for measurement due to the high reactivity of the compound. The Cr $2p_{3/2}$ peak observed in the XPS spectrum of **3′** was assigned to Cr^{3+} with a binding energy of 576.5 eV (Figure 2b). It is assumed that the Cr ions in the compound are originally synthesized as Cr^{2+} and then oxidized to Cr^{3+} in air. The different coordinating ability of the counteranions in the Cr^{2+} precursors is undoubtedly one of the key factors that controls the architectures and reactivity of the compounds.

■ GAS ADSORPTION PROPERTIES

The hydrogen-bonded network in **1**⊃DMF inspired us to investigate its porosity by gas adsorption measurements. Compound **1**⊃DMF was activated at 393 K for 3 h before each gas adsorption measurement. The structure of the compound was retained after the activation process according to the XRPD patterns (Figure S2, Supporting Information). One adsorbs CO_2 (57 mL g^{-1} at 100 kPa, Figure 3a) with a type I isotherm, which is typically found in microporous materials.[14]

The sample could be reused and show similar CO_2 uptake. However, N_2 and O_2 adsorption isotherms measured at 77 K reveal almost no adsorption, which is probably due to the lower kinetics diffusion of N_2 and O_2 in the pores. Changes in the XRPD pattern of the sample were not observed after the gas adsorption experiment, a finding that demonstrates the permanent porosity of the structure. We reason that the hydrogen-bonded network between the nearby pyrazole rings in each unit contributes to the porosity.

Thermogravimetric analysis (TGA) of **2**⊃DMF (Figure S3, Supporting Information) shows unclear weight loss from 298 to 573 K, and the compound is thermally stable up to 573 K, since the decomposition of the ligand occurs above this temperature. The guest species can be removed by heating at 433 K under dynamic vacuum for 16 h. TGA and IR data for the activated sample of **2**⊃DMF (here after denoted as **2**) confirm the removal of DMF molecules from the pores. The XRPD pattern of **2** is different from that of **2**⊃DMF due to the structural transition (Figure 4a). Several peaks are shifted to higher 2θ angles, which suggests closer packing in **2**. The addition of a drop of DMF to **2** could convert the structure back to the original phase, thus demonstrating the reversible structural flexibility of the compound. Gas adsorption experiments were conducted for N_2 (77 K), O_2 (77 K), and CO_2 (195 K) in order to confirm the porosity of **2** (Figure 3b). All adsorption isotherms are type I isotherms without hysteresis between the adsorption and desorption isotherms. The total O_2 uptake (243.6 mL g^{-1} at 18 kPa) is higher than the total N_2 uptake (235.8 mL g^{-1} at 100 kPa) at the same temperature. The total uptake of CO_2 is 181.3 mL g^{-1} at 101 kPa. The Brunauer–Emmett–Teller (BET) surface area of 2 is 700 m^2 g^{-1} as estimated from the N_2 adsorption isotherm.

Uncoordinated DEF molecules in **3**⊃DEF were released up to a maximum temperature of 473 K according to TGA (Figure S3, Supporting Information). Therefore, **3**⊃DEF was slowly

dx.doi.org/10.1021/ic501459m | *Inorg. Chem.* 2014, 53, 9870–9875

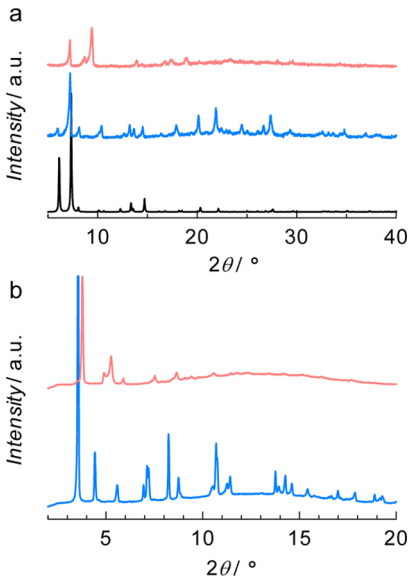

Figure 4. XRPD patterns of (a) simulated **2**⊃DMF (black), **2**⊃DMF (blue), and **2** (red), and (b) **3**⊃DEF (blue) and **3** (red).

heated, and the sample was activated at 453 K for 16 h under vacuum to ensure the removal of the guest molecules from the pores. During heating, the color of the sample changed from the original dark purple to pink and finally dark beige at 453 K. This behavior is due to the structural transformation as evidenced by the XRPD patterns (Figure 4b). Moreover, a similar transformation was also observed in the Cu-based isostructure.[12b] The permanent porosity of **3** was checked by gas adsorption measurement (Figure 3c). Compound **3** adsorbs N_2 at 77 K, but no gas uptake is observed in the Cu-based isostructure.[12b] There are two adsorption steps in the O_2 adsorption isotherm at 77 K, and the first adsorption step occurs at pressures up to 0.7 kPa. O_2 adsorption is reversible, and the sample is reusable without any marked decrease in the gas uptake, thus indicating the weak binding of O_2 in the framework at 77 K.

The high reactivity of **3** in air prompted us to investigate the interaction of **3** with O_2 under ambient conditions. We conducted O_2 adsorption experiments at 298 K (Figure 3d). The O_2 sorption isotherms of **3** revealed the irreversible type I profile with a total amount of 15 mL g^{-1} taken up, while adsorption of N_2 at the same temperature was not observed. The adsorbed O_2 could not be released by simple heating under vacuum, but the porous structure was retained, as indicated by XRPD and O_2 adsorption of **3**′ at 77 K. The irreversible O_2 binding indicates a strong interaction between **3** and O_2 at 298 K without a collapse of the entire porous structure. IR spectra of the compound were recorded during the activation process of **3**⊃DEF. The coordinating DEF, which was linking the two nearby Cr ions, was not removed from the structure during the activation as the C═O stretching frequency was still observed in the spectrum of **3** (Figures 5 and S4, Supporting Information).

The bands at 1671 and 1621 cm^{-1} were observed in the IR spectrum of **3**⊃DEF and assigned for the $\nu_{C=O}$ vibrational mode of free DEF and bridging DEF, respectively. The band of free DEF disappeared during the activation. The peak assigned to the C═O stretching of the coordinating solvent was shifted to 1631 cm^{-1}. The higher wavenumber suggests the weaker coordination bond of DEF.[15] It suggests that the coordination

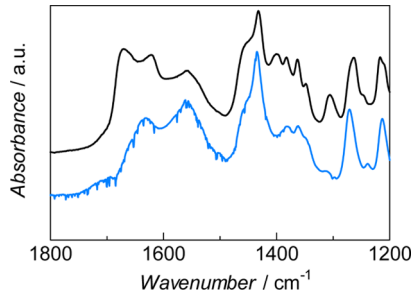

Figure 5. Diffuse reflectance IR spectra of **3**⊃DEF (black) and **3** (blue) recorded at 298 K under vacuum.

bonds between DEF and the Cr centers are partially broken during the activation process and the coordination mode changes from bidentate to monodentate fashion. The monodentate bonding mode of DEF in turn creates some coordinatively unsaturated metal sites in the structure for O_2 binding. Meanwhile, the residual coordinated DEF in the framework plays a role in stabilizing the open framework. We tried various activation conditions to remove all bridging DEF, but the more severe conditions would lead to the collapsing of the structure.

CONCLUSIONS

Three porous Cr-based coordination compounds were synthesized under an Ar atmosphere; one forms a hydrogen-bonded network of discrete complexes, and the others are porous coordination polymers. This is the first report of a Cr-based PCP/MOF with noncarboxylate ligands and characterization by single-crystal X-ray diffraction. A new type of trinuclear Cr−N cluster with 700 m^2 g^{-1} of BET surface area was observed in **2**, and structural flexibility was identified in **2** and **3**. Compound **3** strongly binds O_2 molecules that is attributed to the partial generation of Cr unsaturated sites. This work contributes the synthetic chemistry of Cr-based open frameworks toward gas capture and conversion.

EXPERIMENTAL SECTION

All reactions and manipulations were conducted under an Ar atmosphere except those specifically mentioned. H_2dmcpz[5] and H_2BDT[16] were synthesized by the procedure following the literature. H_2BDT was further acidified to pH 5 by diluted hydrochloric acid and heated at 353 K under vacuum overnight. Deoxidized DMF and methanol (MeOH) were purchased from Wako. DEF was purchased from TCI. All metal precursors were purchased from Sigma−Aldrich. All chemicals were used as commercially available without further purification.

Synthesis of Compounds. Typically, a reaction mixture with a specific ratio was prepared and tightly packed in a glass vial with a Telfon-lined cap. For the air-sensitive product, the sealed glass vial was placed in the O-ring capped metal container to prevent air-contamination during the synthesis.

***1*⊃*DMF*.** $[(CH_3CO_2)_2Cr{\cdot}H_2O]_2$ (0.038 g, 0.1 mmol) and H_2dmcpz (0.112 g, 0.8 mmol) were mixed in a 30 mL glass vial; subsequently, a 1:1 (v/v) mixture of DMF and DEF (10 mL) was added to the solids. The vial was tightly sealed with a Teflon-lined cap and heated in a programmable oven at 393 K for 48 h. Green crystalline solid was filtrated, washed with DMF, and dried under Ar (yield ca. 120 mg). The guest-free sample of **1**⊃DMF (denoted as **1**) was obtained by heating at 393 K for 3 h under vacuum.

***2*⊃*DMF*.** Anhydrous $CrCl_2$ (0.074 g, 0.6 mmol) and H_2BDT (0.129 mg, 0.6 mmol) in 30 mL of DMF was tightly sealed in a 50 mL glass vial and heated at 393 K for 48 h in a programmable oven. Bright-green crystals were collected, washed with DMF, and dried under Ar

dx.doi.org/10.1021/ic501459m | Inorg. Chem. 2014, 53, 9870−9875

(yield ca. 140 mg). Samples for gas adsorption measurements were obtained by heating at 393 K for 16 h under vacuum.

3⊃*DEF*. $[(CH_3CO_2)_2Cr{\cdot}H_2O]_2$ (0.113 g, 0.3 mmol) and H_2BDT (0.514 g, 2.4 mmol) in 30 mL of DEF was tightly sealed in a 50 mL glass vial and heated at 393 K for 24 h. The reaction mixture was slowly cooled to obtain a purple crystalline solid. The product was filtered, washed with DEF, and dried under evacuation (yield ca. 280 mg). The compound is air-sensitive and readily changes its color upon air exposure. Only the air-exposed single crystal (**3′**⊃DEF) was employed for the single-crystal X-ray diffraction. We prepared samples for gas adsorption measurements by heating at 453 K for 16 h under vacuum.

Single-Crystal Structure Determination. The diffraction data were measured at 223 K under N_2 flowing on a Rigaku AFC10 diffractometer with Rigaku Saturn Kappa CCD system equipped with a MicroMax-007 HF/VariMax rotationg-anode X-ray generator with confocal monochromated Mo Kα radiation. All structures were solved by a direct method (SIR-97) and refined by full-matrix least-squares using SHELX-97. Non-hydrogen atoms were refined with anisotropic thermal displacement coefficients. All hydrogen atoms were located on the geometrically ideal positions and refined using a riding model. We note that, for **1**⊃DMF, the hydrogen atom attached to the O4 atom and residues of coordinated solvents were not located in the crystal structure because of strong disordering. The contribution of the missing solvent molecule and other ionic residues to the diffraction patterns of **1**⊃DMF and **2**⊃DMF was subtracted from the reflection data by the SQUEEZE method as implemented in PLATON. The deposited number on the Cambridge Crystallographic Data Centre (CCDC) is 997867.

Other Physical Measurements. XRPD data were collected on a Rigaku RINT 2200 Ultima diffractometer with Cu Kα anode. For synchrotron XRPD data, all air-free samples were carefully sealed in glass capillaries under an Ar atmosphere. XRPD patterns with good count statistics were measured using synchrotron radiation employing a large Debye−Scherrer camera with imaging plate detectors on the BL02B2 beamline at SPring-8. All high-resolution XRPD patterns were obtained using a step size of $2\theta = 0.01°$. The unit cell parameters were refined using a LeBail fitting employing the Rietica software package. Gas adsorption isotherms for all gases were measured by BELSORP-mini equipment. TGA was measured using a Rigaku TG8120 under flowing nitrogen with 10 K min^{-1} ramp rate. Sample preparations for TGA were conducted under air. IR spectra were collected on Thermofisher Scientific Nicolet FT-IR equipped with a gas controller and a temperature controller. Sample was loaded into the sample cell under an Ar atmosphere. We recorded all IR spectra under dynamic vacuum to prevent air contamination during the measurement, and the noise signal on each spectrum is the intrinsic problem from the long-time measurement under evacuation. We used the activated samples for all XPS measurement. All samples were prepared under air so that **3** oxidized to **3′** during the preparation. The measurements were performed on an ULVAC-PHI model 5500 spectrometer with 15 kV, 400W Mg Kα emission as the X-ray source. The charging effect was corrected by adjusting the binding energy of the C 1s peak to be 284.6 eV. For XPS data analysis, the Shirley background was subtracted from each spectrum before the peak fitting. The oxidation state of Cr in all samples was estimated from the Cr $2p_{3/2}$ region. Peak fitting was performed with the Gaussian LorenCross function. We were unable to perform peak deconvolution to analyze on the multiplet splitting effect because of the low resolution of the data.

■ ASSOCIATED CONTENT

Ⓢ Supporting Information

Additional XRPD patterns, TGA profiles, IR spectra, and structural data as a CIF file. This material is available free of charge via the Internet at http://pubs.acs.org.

■ AUTHOR INFORMATION

Corresponding Authors

*(S.H.) E-mail: horike@sbchem.kyoto-u.ac.jp.

*(S.K.) E-mail: kitagawa@icems.kyoto-u.ac.jp.

Notes

The authors declare no competing financial interest.

■ ACKNOWLEDGMENTS

We thank Prof. Yoshiki Kubota for supporting on the synchrotron X-ray diffraction measurements at SPring-8. This work was supported by the PRESTO program of the Japan Science and Technology Agency (JST), a Grant-in-Aid for Scientific Research on the Innovative Areas: “Fusion Materials”, and Grant-in-Aid for Young Scientists (A) from the Ministry of Education, Culture, Sports, Science and Technology, Japan. iCeMS is supported by the World Premier International Research Initiative (WPI), MEXT, Japan.

■ REFERENCES

(1) (a) Chui, S. S.-Y.; Lo, S. M.-F.; Charmant, J. P. H.; Orpen, A. G.; Williams, I. D. *Science* **1999**, *283*, 1148−1150. (b) Li, H.; Eddaoudi, M.; O'Keeffe, M.; Yaghi, O. M. *Nature* **1999**, *402*, 276−279. (c) Yaghi, O. M.; O'Keeffe, M.; Ockwig, N. W.; Chae, H. K.; Eddaoudi, M.; Kim, J. *Nature* **2003**, *423*, 705−714. (d) Kitagawa, S.; Kitaura, R.; Noro, S.-i. *Angew. Chem., Int. Ed.* **2004**, *43*, 2334−2375. (e) Caskey, S. R.; Wong-Foy, A. G.; Matzger, A. J. *J. Am. Chem. Soc.* **2008**, *130*, 10870−10871. (f) Ferey, G. *Chem. Soc. Rev.* **2008**, *37*, 191−214. (g) Murray, L. J.; Dincă, M.; Long, J. R. *Chem. Soc. Rev.* **2009**, *38*, 1294−1314. (h) Zacher, D.; Shekhah, O.; Woll, C.; Fischer, R. A. *Chem. Soc. Rev.* **2009**, *38*, 1418−1429. (i) Farha, O. K.; Hupp, J. T. *Acc. Chem. Res.* **2010**, *43*, 1166−1175. (j) Lin, R.-B.; Li, F.; Liu, S.-Y.; Qi, X.-L.; Zhang, J.-P.; Chen, X.-M. *Angew. Chem., Int. Ed.* **2013**, *52*, 13429−13433. (k) Lu, W.; Wei, Z.; Gu, Z.-Y.; Liu, T.-F.; Park, J.; Park, J.; Tian, J.; Zhang, M.; Zhang, Q.; Gentle Iii, T.; Bosch, M.; Zhou, H.-C. *Chem. Soc. Rev.* **2014**, *43*, 5561−5593.

(2) (a) Cavka, J. H.; Jakobsen, S.; Olsbye, U.; Guillou, N.; Lamberti, C.; Bordiga, S.; Lillerud, K. P. *J. Am. Chem. Soc.* **2008**, *130*, 13850−13851. (b) Dan-Hardi, M.; Serre, C.; Frot, T.; Rozes, L.; Maurin, G.; Sanchez, C.; Férey, G. *J. Am. Chem. Soc.* **2009**, *131*, 10857−10859. (c) Kozachuk, O.; Yusenko, K.; Noei, H.; Wang, Y.; Walleck, S.; Glaser, T.; Fischer, R. A. *Chem. Commun.* **2011**, *47*, 8509−8511. (d) Foo, M. L.; Horike, S.; Inubushi, Y.; Kitagawa, S. *Angew. Chem., Int. Ed.* **2012**, *51*, 6107−6111. (e) Kosaka, W.; Yamagishi, K.; Hori, A.; Sato, H.; Matsuda, R.; Kitagawa, S.; Takata, M.; Miyasaka, H. *J. Am. Chem. Soc.* **2013**, *135*, 18469−18480. (f) Kozachuk, O.; Luz, I.; Llabrés i Xamena, F. X.; Noei, H.; Kauer, M.; Albada, H. B.; Bloch, E. D.; Marler, B.; Wang, Y.; Muhler, M.; Fischer, R. A. *Angew. Chem., Int. Ed.* **2014**, *53*, 7058−7062.

(3) (a) Serre, C.; Millange, F.; Thouvenot, C.; Noguès, M.; Marsolier, G.; Louër, D.; Férey, G. *J. Am. Chem. Soc.* **2002**, *124*, 13519−13526. (b) Férey, G.; Mellot-Draznieks, C.; Serre, C.; Millange, F.; Dutour, J.; Surblé, S.; Margiolaki, I. *Science* **2005**, *309*, 2040−2042. (c) Surblé, S.; Millange, F.; Serre, C.; Düren, T.; Latroche, M.; Bourrelly, S.; Llewellyn, P. L.; Férey, G. *J. Am. Chem. Soc.* **2006**, *128*, 14889−14896. (d) Surble, S.; Serre, C.; Mellot-Draznieks, C.; Millange, F.; Ferey, G. *Chem. Commun.* **2006**, *0*, 284−286. (e) Murray, L. J.; Dincă, M.; Yano, J.; Chavan, S.; Bordiga, S.; Brown, C. M.; Long, J. R. *J. Am. Chem. Soc.* **2010**, *132*, 7856−7857.

(4) (a) Brozek, C. K.; Dincă, M. *J. Am. Chem. Soc.* **2013**, *135*, 12886−12891. (b) Liu, T.-F.; Zou, L.; Feng, D.; Chen, Y.-P.; Fordham, S.; Wang, X.; Liu, Y.; Zhou, H.-C. *J. Am. Chem. Soc.* **2014**, *136*, 7813−7816.

(5) Montoro, C.; Linares, F.; Quartapelle Procopio, E.; Senkovska, I.; Kaskel, S.; Galli, S.; Masciocchi, N.; Barea, E.; Navarro, J. A. R. *J. Am. Chem. Soc.* **2011**, *133*, 11888−11891.

(6) Zhang, J.-P.; Zhang, Y.-B.; Lin, J.-B.; Chen, X.-M. *Chem. Rev.* **2012**, *112*, 1001−1033.

(7) (a) Chang, S. C.; Jeffrey, G. A. *Acta Crystallogr., Sect. B: Struct. Crystallogr. Cryst. Chem.* **1970**, *26*, 673−683. (b) Cotton, F. A.; Wang, W. *Inorg. Chem.* **1982**, *21*, 2675−2678.

(8) (a) Steiner, T. *J. Chem. Soc., Chem. Commun.* **1995**, 1331−1332. (b) Arunan, E.; Desiraju, G. R.; Klein, R. A.; Sadlej, J.; Scheiner, S.; Alkorta, I.; Clary, D. C.; Crabtree, R. H.; Dannenberg, J. J.; Hobza, P.; Kjaergaard, H. G.; Legon, A. C.; Mennucci, B.; Nesbitt, D. J. *Pure Appl. Chem.* **2011**, *83*, 1637−1641.
(9) Herr, R. J. *Bioorg. Med. Chem.* **2002**, *10*, 3379−3393.
(10) (a) Figgis, B. N.; Robertson, G. B. *Nature* **1965**, *205*, 694−695. (b) Cannon, R. D.; Jayasooriya, U. A.; Sowrey, F. E.; Tilford, C.; Little, A.; Bourke, J. P.; Rogers, R. D.; Vincent, J. B.; Kearley, G. J. *Inorg. Chem.* **1998**, *37*, 5675−5677. (c) Ng, V. W. L.; Kuan, S. L.; Leong, W. K.; Koh, L. L.; Tan, G. K.; Goh, L. Y.; Webster, R. D. *Inorg. Chem.* **2005**, *44*, 5229−5240. (d) Figuerola, A.; Tangoulis, V.; Ribas, J.; Hartl, H.; Brüdgam, I.; Maestro, M.; Diaz, C. *Inorg. Chem.* **2007**, *46*, 11017−11024. (e) Schoedel, A.; Zaworotko, M. J. *Chem. Sci.* **2014**, *5*, 1269−1282.
(11) (a) Allen, F. *Acta Crystallogr., Sect. B: Struct. Sci.* **2002**, *58*, 380−388. (b) Bruno, I. J.; Cole, J. C.; Kessler, M.; Luo, J.; Motherwell, W. D. S.; Purkis, L. H.; Smith, B. R.; Taylor, R.; Cooper, R. I.; Harris, S. E.; Orpen, A. G. *J. Chem. Inf. Comput. Sci.* **2004**, *44*, 2133−2144.
(12) (a) Tao, J.; Ma, Z.-J.; Huang, R.-B.; Zheng, L.-S. *Inorg. Chem.* **2004**, *43*, 6133−6135. (b) Dincă, M.; Yu, A. F.; Long, J. R. *J. Am. Chem. Soc.* **2006**, *128*, 8904−8913. (c) Ouellette, W.; Prosvirin, A. V.; Whitenack, K.; Dunbar, K. R.; Zubieta, J. *Angew. Chem., Int. Ed.* **2009**, *48*, 2140−2143. (d) Demessence, A.; Long, J. R. *Chem.—Eur. J.* **2010**, *16*, 5902−5908. (e) Deng, J.-H.; Yuan, X.-L.; Mei, G.-Q. *Inorg. Chem. Commun.* **2010**, *13*, 1585−1589. (f) Liu, W.-T.; Ou, Y.-C.; Lin, Z.-j.; Tong, M.-L. *CrystEngComm* **2010**, *12*, 3487−3489. (g) Sumida, K.; Foo, M. L.; Horike, S.; Long, J. R. *Eur. J. Inorg. Chem.* **2010**, *2010*, 3739−3744. (h) Zhong, D.-C.; Feng, X.-L.; Lu, T.-B. *CrystEngComm* **2011**, *13*, 2201−2203. (i) Liu, W.-T.; Li, J.-Y.; Ni, Z.-P.; Bao, X.; Ou, Y.-C.; Leng, J.-D.; Liu, J.-L.; Tong, M.-L. *Cryst. Growth Des.* **2012**, *12*, 1482−1488. (j) Yan, Z.; Li, M.; Gao, H.-L.; Huang, X.-C.; Li, D. *Chem. Commun.* **2012**, *48*, 3960−3962.
(13) Steinberger, R.; Duchoslav, J.; Arndt, M.; Stifter, D. *Corros. Sci.* **2014**, *82*, 154−164.
(14) Sing, K. S. W. *Pure Appl. Chem.* **1985**, *57*, 603−619.
(15) Nakamoto, K. Applications in Coordination Chemistry. In *Infrared and Raman Spectra of Inorganic and Coordination Compounds*; John Wiley & Sons, Inc.: Hoboken, NJ, 2008.
(16) Vereshchagin, L. I.; Petrov, A. V.; Proidakov, A. G.; Pokatilov, F. A.; Smirnov, A. I.; Kizhnyaev, V. N. *Russ. J. Org. Chem.* **2006**, *42*, 912−917.